

SHORT ECHO TIME SINGLE VOXEL  
MAGNETIC RESONANCE SPECTROSCOPY  
IN THE CHARACTERISATION OF  
CHILDHOOD BRAIN TUMOURS

by

LISA MARIA HARRIS

A thesis submitted to  
The University of Birmingham  
for the degree of  
DOCTOR OF PHILOSOPHY

Institute of Child Health  
Medical School  
The University of Birmingham  
June 2009

UNIVERSITY OF  
BIRMINGHAM

**University of Birmingham Research Archive**

**e-theses repository**

This unpublished thesis/dissertation is copyright of the author and/or third parties. The intellectual property rights of the author or third parties in respect of this work are as defined by The Copyright Designs and Patents Act 1988 or as modified by any successor legislation.

Any use made of information contained in this thesis/dissertation must be in accordance with that legislation and must be properly acknowledged. Further distribution or reproduction in any format is prohibited without the permission of the copyright holder.

# **ABSTRACT**

## **INTRODUCTION**

Brain tumours are the most common solid tumour in childhood, while Magnetic Resonance Spectroscopy (MRS) studies have been performed on brain tumours previously, the majority have been performed on the adult patient population and at long echo times. The work presented in this thesis outlines work performed in the usage of short echo time MRS in the characterisation of childhood brain tumours.

## **METHODS**

Short echo time MRS was performed on children with brain tumours at the time of diagnostic imaging. In addition, follow up data was accrued for some patients. Resulting spectra were assessed for characteristics either of diagnosis, prognosis or treatment response.

## **RESULTS**

Spectra collected were used in assessing characteristics of an array of childhood brain tumours. Initially the technique was tested on a well understood dataset of cerebellar tumours, and was later expanded to provide diagnostic aids for both brain stem tumours and pineal region tumours. A group of pilocytic astrocytomas were assessed for differences by location within the brain, for prognosis and for response to treatment.

## **CONCLUSIONS**

The additional information given by short echo time MRS was useful in the characterisation of childhood brain tumours.

## **Dedication**

This thesis is dedicated to my parents, who offered me unconditional love and support all the way since the beginning of my studies.

## **ACKNOWLEDGEMENTS**

There are a large number of people I would like to thank, and without whom this thesis is unlikely to have been written.

I would like to thank all my former colleagues from the Institute of Child Health and Electrical, Electronic and Computer Engineering. I would especially like to thank both of my supervisors, Dr Andrew Peet and Dr Theodoros Arvanitis, whose assistance, enthusiasm and encouragement helped me in all stages of my PhD. I would also like to thank Nigel Davies, Martin Wilson and Greg Reynolds for vast amounts of patience with helping me to learn computer programming. Additional thanks goes to Yu Sun, Kal Natarajan and Alex Gibb. Additional thanks goes out to everyone who made the department run smoothly.

I would like to thank the radiology team at BCH, especially Dr Lesley MacPherson and Shaheen Lateff. Thanks also goes out to all those involved in this study at the Royal Marsden Hospital (Sutton), Great Ormond Street Hospital and Queen's Medical Centre.

I offer warm thanks to both Martin Wilson and John Easton for offering a sounding board for ideas, listening to me complain when some of them didn't work and providing a near endless supply of coffee!

I would like to thank Alan Wright and Richard Harrison for proof reading my thesis, and correcting numerous grammatical errors.

I would like to thank all of my family for their unconditional love and support throughout both my research and the writing up of this thesis. I cannot state how much I would like to thank my parents for their support and encouragement at all stages of my education. They supported me both emotionally and financially for so long and without them I cannot see that this PhD would have been possible. I would like to thank my grandparents for their limitless encouragement and for believing in me when even I didn't! I would like to thank all my extended family, especially my cousins, Amanda and Carolyn, for always being there to listen when I needed them to.

I offer heartfelt thanks to all my housemates over the duration of my PhD. Massive amounts of gratitude goes out to Helen and Nicole, for always knowing when chocolate/wine/DVD night was required.

I would like to thank all of my friends, for listening, encouraging and for always making me laugh when things were going less than well. I would like to warmly thank Martina, Ben, Seema, Mischa, Alan, Nic, 'Ien, Daf and Ellen.

I would like to offer huge thanks to Sean, for giving me so much love and support, and providing me with sanity, chocolate and dancing!

Finally I would like to thank all of my new colleagues at the University of Surrey for their support in the final stages of writing up.

## **DECLARATION**

I confirm that this work is my own and that I have been involved in the design and conduct of these studies, analysis of data and preparation of this thesis. The following aspects of these studies were undertaken as part of collaboration.

Data was collected from four hospitals: Birmingham Children's Hospital; The Royal Marsden Hospital (Sutton); Queen's Medical Centre (Nottingham); and Great Ormond Street Hospital (London). The staff of the radiology departments in these hospitals were responsible for collecting magnetic resonance imaging and spectroscopy data. Histopathology was undertaken by the pathology department within each hospital.

Data analysis was performed by the author, with some additional programming assistance given by Dr Nigel Davies, Dr Martin Wilson and Dr Gregory Reynolds.

High resolution in vitro MRS was performed and analysed by Dr Martin Wilson.

The multi-centre radiology review of brain stem tumours was performed by Dr Lesley MacPherson, Dr Dawn Saunders and Dr Tim Jaspan.

# **CONTENTS**

## CHAPTER 1: INTRODUCTION

- 1.1 Brain Tumours in Children
- 1.2 Methods for Diagnosing Childhood Brain Tumours
  - 1.2.1 Histopathology
  - 1.2.2 Magnetic Resonance Imaging (MRI)
  - 1.2.3 Blood Markers for Diagnosis
  - 1.2.3 New Imaging Techniques
- 1.3 Tumour Types
  - 1.3.1 Glial Tumours
  - 1.3.2 Primitive Neuroectodermal Tumours (PNETs)
  - 1.3.3 Germ Cell Tumours (GCTs)
  - 1.3.4 Other Tumours
- 1.4 Tumour locations
  - 1.4.1 Distribution
  - 1.4.2 Cerebellar Tumours
  - 1.4.3 Brain Stem Tumours
  - 1.4.4 Pineal Region Tumours
  - 1.4.5 Optic Pathway Tumours and NF1
- 1.5 Current State of MRS
- 1.6 Current uses of MRS in Brain Tumour Research

## CHAPTER 2: MAGNETIC RESONANCE SPECTROSCOPY

- 2.1 Theory of the NMR Phenomenon
- 2.2 Magnetic Resonance Spectroscopy (MRS)
- 2.3 Clinical MRS
  - 2.3.1 Pulse Sequences
  - 2.3.2 Water Suppression
  - 2.3.3 MRS Signal Pre-processing
  - 2.3.4 Types of MRS Localisation
  - 2.3.5 Echo Times
  - 2.3.6 Functions of Different Metabolites
- 2.4 Analysis Tools
- 2.5 Extensions
- 2.6 Challenges of <sup>1</sup>H MRS
- 2.7 Summary

## AIMS AND OBJECTIVES

## OVERVIEW OF RESULTS

## CHAPTER 3: METHODS

- 3.1 EXPERIMENTAL PROTOCOLS
- 3.2 ANALYSIS METHODS
  - 3.2.1 Pre-Processing and Processing
  - 3.2.2 Quality Control
  - 3.2.3 Analysis Using Spectra Produced by Scanner Software
  - 3.2.4 Analysis Using Metabolite Concentrations

### 3.3 STATISTICAL METHODS FOR THE INTERPRETATION OF RESULTS

#### CHAPTER 4: CEREBELLAR TUMOURS

##### 4.1 INTRODUCTION

##### 4.2 A DIAGNOSTIC SCHEME BASED ON MRS PEAK HEIGHTS

4.2.1 A Diagnostic Scheme based on MRS Peak Heights from Retrospective Analysis

4.2.2 Prospective Evaluation of Peak Height Classifier

4.2.3 Updating and Extending the Peak Height Classifier

4.2.4 Summary

##### 4.3 A DIAGNOSTIC SCHEME BASED ON LCMODEL™ METABOLITE CONCENTRATIONS

4.3.1 An enhanced diagnostic scheme based on metabolite concentrations determined from retrospective analysis

4.3.2 An enhanced diagnostic scheme based on metabolite concentrations determined from retrospective analysis using a full set of metabolite concentrations

4.3.3 Prospective Evaluation – diagnostic scheme based on metabolite concentrations

##### 4.7 SUMMARY OF MAIN FINDINGS AND CONCLUDING REMARKS

#### CHAPTER 5: PINEAL REGION TUMOURS

##### 5.1 INTRODUCTION

##### 5.2 METHODS AND PATIENTS

##### 5.3 RESULTS

##### 5.4 DISCUSSION

##### 5.5 CONCLUSION

#### CHAPTER 6 BRAIN STEM TUMOURS

##### 6.1 INTRODUCTION

##### 6.2 METHODS AND PATIENTS

##### 6.3 RESULTS

##### 6.4 DISCUSSION

##### 6.5 CONCLUSION

#### CHAPTER 7: PILOCYTIC ASTROCYTOMAS: SPECTRAL VARIATION WITH LOCATION AND PROGRESSION

##### 7.1 INTRODUCTION

##### 7.2 METHODS

##### 7.3 RESULTS

7.3.1 Differences in MRS metabolite Profiles between Cerebellar and Supratentorial Tumours

7.3.2 Pre-Treatment MRs as a Prognostic Indicator in Supratentorial Tumours

7.3.3 Supratentorial Tumours: Treatment Monitoring and Early Predictors of Progression

##### 7.4 DISCUSSION

##### 7.5 CONCLUSION

CHAPTER 8: CONCLUSIONS

REFERENCES

## LIST OF ILLUSTRATIONS

Figure 1: Pie chart depicting the cause of death in children under the age of 15 years, in the year 2007

Figure 2: Pie Chart depicting the distribution of deaths from cancers in children under the age of 15 years, in the year 2007

Figure 3: Labelled side view of the brain

Figure 4: Synthesised in vivo  $^1\text{H}$ -MR spectrum

Figure 5: Lactate

- a) Molecular structure
- b)  $^1\text{H}$  MR spectrum

Figure 6: PRESS sequence

Figure 7: Examples of  $^1\text{H}$ -MR spectra at different echo times:

- a) TE = 135ms
- b) TE = 30ms

Figure 8: Synthesised spectra for individual metabolites

- a) N-Acetyl Aspartate and N-Acetyl Aspartyl-glutamate
- b) Glycerophosphocholine and Phosphocholine
- c) Creatine
- d) Myo-Inositol
- e) Scyllo-Inositol
- f) Glycine
- g) Lactate
- h) Taurine

Figure 9: Voxel placement for a cerebellar tumour

- a) Axial plane
- b) Sagittal plane

Figure 10: Example of a  $^1\text{H}$ -MR spectrum processed by the Siemens' Symphony NUM4 software

Figure 11: Examples of poor quality  $^1\text{H}$ -MR spectra

- a) An example with broad lines
- b) An example with very low SNR.

Figure 12: 2 step classification scheme for cerebellar tumours based on peak height ratio measurement – retrospective study of cerebellar tumours using peak height ratios

Figure 13: Peak height classification scheme measurement – retrospective study

Figure 14: Flow diagram showing the analysis of multicentre data

Figure 15: Average spectra for the three main cerebellar tumours

Figure 16: Prospective evaluation of the peak height classification scheme – new cases on the original classification axes

Figure 17: 2 step classification scheme for cerebellar tumours based on peak height ratio measurement – using the full, multicentre data set

Figure 18: Peak height classification scheme measurement – using the full, multicentre data set

Figure 19: Plot showing cerebellar tumour separation on the axes tNAA/Cr Vs mIns/tCho – using LCMoDel™ generated metabolite concentrations

Figure 20: Principal Component Analysis of cerebellar tumours – using LCMoDel™ generated metabolite concentrations

Figure 21: Plot showing cerebellar tumour separation on the axes tCho Vs mIns – using LCMoDel™ generated metabolite concentrations

Figure 22: Bar charts showing the average (a) metabolite and (b) LMM concentrations for each of the 3 major tumour types of the cerebellum, as determined from LCMoDel™

Figure 23: Prospective evaluation of the metabolite classification scheme – the full, multicentre data set on the axes tCho Vs mIns

Figure 24: Bar charts showing metabolite (a) and LMM (b) concentrations of rare tumours of the cerebellum compared with those found in the 3 major tumour groups of the cerebellum

Figure 25: Average spectra for pineal region tumours

Figure 26: Germ Cell Tumours and other pineal region tumours plotted on axes for LMM regions at 0.9ppm and 1,3ppm

Figure 27: Germ cell tumours plotted on axes tCho Vs Cr

Figure 28: Average spectra for brain stem tumours

Figure 29: Principal Component Analysis of brain stem tumours

Figure 30: Brain stem tumours plotted on axes mIns/tCho Vs Cr/tCho

Figure 31: Diffuse gliomas within and extending beyond the pons plotted on axes for the LMM regions (relative to tCho) at 0.9ppm and 1.3ppm

Figure 32: Bar charts showing (a) metabolite and (b) LMM concentrations (relative to total Cho) for brain stem tumour

Figure 33: Pie chart depicting pilocytic astrocytoma distribution within the brain

Figure 34: Mean spectra for pilocytic astrocytoma by location

Figure 35: Principal Component Analysis of pilocytic astrocytoma by location

Figure 36: Pilocytic astrocytoma, separated by location, plotted on the axes mIns Vs Glx

## **LIST OF TABLES**

- Table 1: Patient information for retrospective study of scanner produced spectra of cerebellar tumours
- Table 2: AUC values for retrospective study of scanner produced spectra of cerebellar tumours
- Table 3: Classification Rates for prospective evaluation of classification scheme for cerebellar tumours, based on peak height measurement from spectra produced by MR scanner software
- Table 4: T-Test results for re-optimising the classification scheme for cerebellar tumours based on spectra from the scanner software
- Table 5: AUC values for prospective study of scanner produced spectra of the three main cerebellar tumour types
- Table 6: Classification of cerebellar tumours using a multicentre dataset, using peak height measurement
- Table 7: Peak height ratios of rare cerebellar tumours
- Table 8: Classification of rare tumours of the cerebellum using the revised peak height classifier
- Table 9: ANOVA and AUC results for using ratios of LCModel™ derived metabolite concentrations, in the classification of cerebellar tumours
- Table 10: Average metabolite values for each cerebellar tumour type and ANOVA results using a full LCModel™ basis set
- Table 11: T-test results and AUC values for building a 2-step classification scheme using metabolite concentrations.
- Table 12: Comparison of classification rates of the different schemes for classifying cerebellar tumours
- Table 13: Average metabolite and LMM concentrations for pineal region tumours
- Table 14: T-test results for comparison between germ cell tumours of the pineal region and pineal parenchymal tumours
- Table 15: P-values for the comparison of germinoma metabolite concentrations with other germ cell tumours of the pineal region
- Table 16: Diagnosis summary for patients in the brain stem tumour study

Table 17: T-Test results for comparison of brain stem tumours

Table 18: Average metabolite values for each brain stem tumour type and ANOVA results using a full LCModel™ basis set

Table 19: P-values and averages for comparison between cerebellar and supratentorial pilocytic astrocytoma

Table 20: P-Value and average metabolite values for determination of progression of supratentorial pilocytic astrocytoma from pre-treatment MRS

## LIST OF ABBREVIATIONS

Ala – alanine  
Asp – aspartate  
ATRT – Atypical Teratoid/Rhabdoid Tumour  
BCH – Birmingham Children’s Hospital  
CCLG – Children’s Cancer and Leukaemia Group  
Cho - choline  
CNS – central nervous system  
Cr – creatine  
CRLB – cramer-rao lower bound  
CSF – cerebrospinal fluid  
CSI – chemical shift imaging  
CT – computed tomography  
DG – diffuse glioma  
DPG – diffuse pontine glioma  
DTI – diffusion tensor imaging  
DWI – diffusion weighted imaging  
FID – free induction decay  
FWHM – full width at half maximum  
GCT – germ cell tumours  
Glc – glucose  
Gln – glutamine  
Glu – glutamate  
Glx – glutamine + glutamate  
Gly – glycine  
GM – grey matter  
GOSH – Great Ormond Street Hospital  
GPC – glycerophosphocholine  
Gua - guanadinoacetate  
HCG – human chorionic gonadotropin  
HGG – high grade glioma  
Lac – lactate  
LGG – low grade glioma  
LMM – lipids + macromolecules  
mIns – myo-inositol  
MMP-2 - matrix metalloproteinase 2  
MR – magnetic resonance  
MRI – magnetic resonance imaging  
MRS – magnetic resonance spectroscopy  
MRSI – magnetic resonance spectroscopic imaging  
NAA – n-acetyl-aspartate  
NAAG – n-acetyl-aspartyl-glutamate  
NF1 – neurofibromatosis type 1  
PA – pilocytic astrocytoma  
PC – principal component  
PCA – principal component analysis  
PCh – phosphocholine  
PCr - phosphocreatine  
ppm – parts per million

PPT – pineal parenchymal tumour  
QMC – Queen’s Medical Centre (Nottingham)  
RMH – Royal Marsden Hospital  
sIns – scyllo-inositol  
SNR – signal-to-noise ratio  
SVS – single voxel spectroscopy  
Tau – taurine  
tCho – total choline  
TE – echo time  
tNAA – NAA + NAAG  
TPG – tectal plate glioma  
TR – repetition time  
VOI – volume of interest  
WHO – World Health Organisation  
WM – white matter

# CHAPTER 1: INTRODUCTION

## 1.1 BRAIN TUMOURS IN CHILDREN

Although cancer is very rare in childhood, with less than 1% of all cancers registered in 2005 being from children [1], it is the most common cause of death from disease in children over one year of age (figure 1).

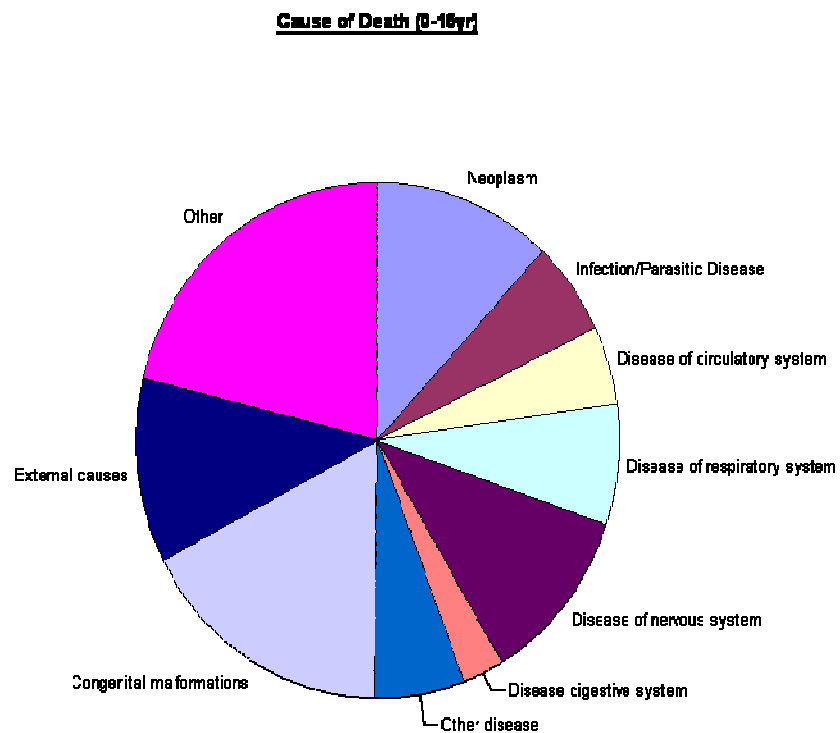


*Figure 1: Pie chart depicting cause of death in children under the age of 15 years in the year 2007 [1]*

### **Prevalence of Different Types of Cancer (<16yr)**

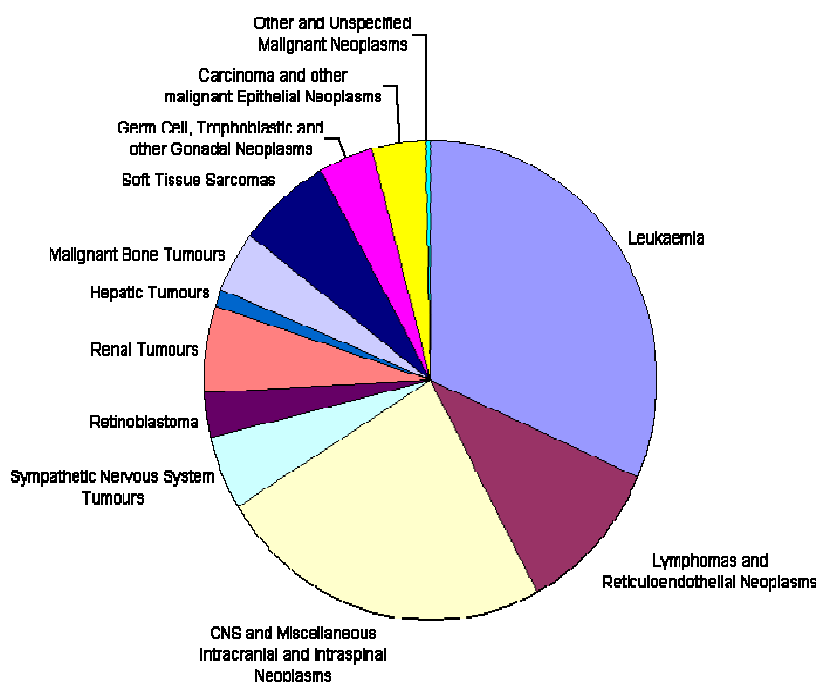


*Figure 2: Pie Chart depicting the distribution of deaths from cancers in children under the age of 15 years, in the year 2007 [1]*

Of all cancers that can occur in childhood, brain tumours are the commonest type of solid tumour (figure 2), with 24% of registered cancer being in the CNS [2]. The only cancer more prevalent in childhood is leukaemia, with a reported 31% of registered cancers being attributed to this in 2000. In the year 2000, 340 new CNS tumours were diagnosed in the UK [2], out of an overall 1426 reported. Survival rates of childhood cancer in the UK have improved overall over time, with an overall survival of 33% in the period 1962-1971 increasing to 73% in the period 1992-1996 [2]. The survival in CNS tumours has increased from 38% to 66% in the same period. Improved and earlier diagnosis and characterisation is vital in the continuation of this trend.

## **1.2 METHODS FOR DIAGNOSING CHILDHOOD BRAIN**

### **TUMOURS**

When a child has a suspected brain tumour, one of the first and most important procedures performed is either a CT or MRI scan. This then confirms the presence, or absence, of a tumour. A CT examination is quicker and cheaper to perform and many types of brain tumours will appear on these images. MRI is often preferred as it has much more detail present and most brain tumours will be apparent on these scans. It can essentially be used to confirm or remove the likelihood of a brain tumour being present in a child exhibiting symptoms indicating the presence. Conventional MRI can be used to detect the presence of abnormalities in the brain, but it is usually not enough to determine the type of tumour present. This is achieved by performing a biopsy and histopathology.

#### **1.2.1 HISTOPATHOLOGY**

Histopathology is a microscopic examination of a biopsy sample in order to assess the presence and type of disease. It is the current 'gold standard' for the diagnosis of brain tumour type and grade.

Once the tissue has been removed, it needs to be stabilised by fixing it in formalin. It is then embedded into paraffin, which allows for very thin slices to be cut and these can then be processed and assessed through staining. To assess the tissue sample, the slices are stained with a variety of stains, which reveal cellular components and allow contrast. A combination of hematoxylin

and eosin is used to stain the nuclei blue and the cytoplasm pink, which allows the cellular structure to be assessed [3].

There are many other stains, which allow highlighting of different features and categories of cells under the microscope using the technique of immunohistochemistry. Immunohistochemistry allows for the staining of proteins and lipids using antibodies of specific types. One example of this is the presence of glial fibrillary acidic protein (GFAP); this is found in glial cells such as astrocytes. A common stain used is for the Ki-67 protein, this is a marker of cell proliferation. As such, this is highly elevated in cells which have a fast turnover, and thus elevated in tumour tissue. This is one of the methods used to grade tumours, and in the assessment for aggressiveness and invasion. The stain MIB-1 is most commonly used to stain for this protein and is used to determine the Ki-67 labelling index of a sample, which is higher in more aggressive tumours [4].

The use of histopathology and immunohistochemistry allows for a definitive diagnosis of the tumour. This is not always achievable in cases of small specimens that may be lacking in viable tumour tissue [5], but we can normally obtain a diagnosis using this method. This is further complicated when there is not complete concordance between histopathologists, and in some cases an agreement between histopathologists is difficult.

There are risks associated with the surgery necessary for obtaining the tumour tissue sample [5-7]. This is not always required as part of a treatment

plan for a patient. Some of these tumours do not require surgical intervention because of their benign nature, meaning that watching these tumours would be preferable. Other tumours are less amenable to surgery, but do respond to other treatments available. An example of the latter would be a germinoma; these grow back rapidly post-operatively, but are exquisitely sensitive to radiotherapy [8, 9]. These tumours are located in the midline of the brain, for example in the pineal region, which is a highly delicate area to biopsy, and would therefore benefit from surgery not being performed unnecessarily.

Characterising tumours, which are within a set group, creates further limitations concerning histopathological diagnosis. Two particular tumours may be given an identical diagnosis due to an identical histopathological appearance, but each may respond differently to certain treatments or, alternatively, one may be significantly more aggressive than the other. It may not be possible to detect these subtle differences using standard histopathology and immunohistochemistry [10]. Much interest has been generated into the discovery of novel biomarkers which have the ability to give additional information about the tumour's behaviour and, in particular, prognosis

In addition, to obtain the best resection, it would benefit the surgeon to know a diagnosis prior to surgery. This information could be used to plan the resection extent.

### **1.2.2 BLOOD MARKERS OF DIAGNOSIS**

There are a small number of tumours which secrete substances into the blood which, if detected, can be used for diagnosis. The main example of tumours where this is present is germ cell tumours, which may secrete alpha-fetoprotein and Beta HCG.

### **1.2.3 MRI**

MRI has been used in the assessment of brain tumours for many years. It is often the first imaging procedure performed when a brain tumour is suspected. It is non-invasive and may offer a means to determine a diagnosis pre-surgically. In tumours where surgery is very high risk, for example those located within the brain stem, it forms a major part of the final diagnosis [11].

Diagnosis using MRI is achieved using certain features such as the location of the tumour with a high accuracy [12, 13], whether it has metastasised and whether there is a cyst present. Other features such as being iso-dense or hypo-dense are also considered, as is the apparent invasion of surrounding tissue [14].

### **1.2.4 NEW IMAGING TECHNIQUES**

Newer imaging techniques often used in the assessment of a suspected brain tumour include diffusion weighted imaging (DWI), diffusion tensor imaging (DTI) AND magnetic resonance spectroscopy (MRS).

### *DIFFUSION WEIGHTED IMAGING*

DWI is a modification of standard MRI techniques, and allows for the measurement of random motion of molecules. From this, images can be weighted with characteristics of water diffusion. This has been shown to be useful for the differentiation between brain abscesses, cystic and non-cystic tumours [15-17].

### *DIFFUSION TENSOR IMAGING*

DTI is an MR technique that enables the measurement of the restricted diffusion of water in tissues. This allows for the imaging of neural tracts. DTI can be used to perform tractography within white matter, where fibres can be tracked along their entire length [18-26]. This is a useful tool for measuring deficits in the white matter, and has been used in the assessment of white matter lesions, such as those caused by trauma ([19, 21, 23]. DTI has also been used in the assessment of tumours [18, 20, 22, 24-26], including in surgical planning [18, 22, 25, 26] and determining recurrence [20, 24].

### *MAGNETIC RESONANCE SPECTROSCOPY*

MRS is a technique that allows for the non-invasive assessment of the metabolites present in a given volume of tissue using an MR scanner. A region of interest is selected either in the tumour or in a region of suspicion. A cubic region is selected, called a voxel, and this is the region which the spectrum is depicting. This can either be performed using one region of interest (single voxel spectroscopy – SVS) or a grid of many voxels (magnetic resonance spectroscopic imaging – MRSI or chemical shift imaging – CSI).

This has been shown to be useful in the assessment of a variety of conditions, including brain tumours [27-30], brain injury [31-34], and a variety of neurological conditions [35].

## **1.3 TUMOUR TYPES**

Tumours that occur in children are mainly different to those occurring in the adult population, with some tumour types being unique to the paediatric population. These are usually classified by the WHO classification system of 2007 [36].

### **1.3.1 GLIAL TUMOURS**

The glial group of tumours is a diverse group, derived from astrocytes, oligodendroglial cells, and ependyma [37]: astrocytomas, ependymomas and, in rare instances, oligodendrogliomas. Each of these has a very different prognosis and requires different treatment plans.

#### *ASTROCYTOMAS*

Astrocytomas are one of the subgroups of gliomas, unbiopsied astrocytomas are usually referred to as gliomas. Astrocytomas can vary in aggression and prognosis, ranging from slow growing (WHO grade 1; pilocytic astrocytoma (PA)) to very fast growing, highly invasive (WHO grade 4; glioblastoma multiforme (GBM)).

In the adult patient population higher grade astrocytomas are common, but these are rare in children. The majority of astrocytomas diagnosed in children

are PAs [38], which have a Ki67 usually <5% [39, 40], with a 10 year survival rate greater than 85% [41].

Diffuse gliomas do not carry such a good outlook; these are common in the brain stem. Diffuse intrinsic brainstem gliomas comprise 15-20% of all CNS tumours in children [42]. These are one of the main causes of death in children with brain tumours, with more than 90% of those diagnosed dying within 2 years of diagnosis [42]. Since biopsy carries a significant risk they are commonly diagnosed on clinical and imaging grounds alone, restricting the opportunity for biological studies.

Higher grade gliomas can also occur in children, but these are less common, comprising approximately 5% of childhood brain tumours. These are more common in the adult population, where they carry an extremely poor prognosis. However, in children, although the prognosis is still poor, even patients with grade IV lesions can become long term survivors implying that these lesions are different biologically than those found in adults.

### *EPENDYMOMA*

Ependymomas are the third most common brain tumour in children [41, 43], and are especially common in younger children, with the average age of diagnosis being less than 6 years [43, 44]. As with astrocytomas, these tumours can have a spectrum of grades from WHO grade 1 to 3 [45, 46]. Grade 1 ependymomas occur predominantly in the spine. Grades 2 and 3 can occur both infratentorially and supratentorially, these form a continuum

and the distinction between these is controversial. However, they are more common in the posterior fossa [45] and this percentage is increased in childhood ependymomas.

### **1.3.2 PRIMITIVE NEUROECTODERMAL TUMOURS (PNET)**

PNETs are aggressive tumours, corresponding to WHO grade 4; these tumours have a tendency towards metastasising. They can occur both infra- and supra-tentorially, those occurring supratentorially are referred to as supratentorial PNETs (SPNETs), or pineoblastomas when located in the pineal region. Those occurring infratentorially are referred to as medulloblastomas. PNETs in the posterior fossa are the most common, with medulloblastomas comprising 20-25% of all childhood brain tumours reported [47]. SPNETs are much less common, comprising <3% [47].

These tumours have similar appearances on histology, but SPNETs have been shown to carry a worse prognosis than medulloblastomas [47, 48], with a markedly lower 5 year recurrence free survival [47]. Another important prognostic factor with these tumours is the presence of metastases. These have a huge impact on the 5 year overall free survival rates, with 1 study quoting a drop from 87.2% to 25.0% in the presence of metastatic spread [47].

### **1.3.3 GERM CELL TUMOURS (GCTs)**

These tumours are thought to arise from primordial germ cells and account for about 3% of cancers in children. They most commonly occur in the testes or

ovaries, but can occur intracranially. Intracranial GCTs are more common in children than in adults [49]. They occur in the midline, mainly in the pineal or suprasellar regions of the brain. Intracranial GCTs comprise <5% of all brain tumours [9], although this is higher in Japan and the Far east. They are a highly diverse group, ranging from the benign to the highly malignant. There are 3 main subgroups of GCT: germinomas; secretory GCTs (SGCTs); and teratomas. Germinomas are the most common [9], despite being highly aggressive tumours they are highly radiosensitive [9, 50] and, hence, carry a good prognosis with quoted 5 year progression free survival rates often in excess of 90% [8, 9, 51-53]. Around 25% of intracranial GCTs are secretory [8, 9, 49, 50, 52]; these are diagnosed on the basis of serum markers [9, 49]. These are highly malignant and less sensitive to radiotherapy than germinomas [9, 52]. This leads to a worse prognosis, with an event free survival of 5-years being approximately 50% [9, 52, 53]. The remaining 10% of intracranial GCTs are variants of teratoma. These can be either benign (mature teratoma) or malignant (immature teratoma) [54]. There is a good prognostic outcome for patients with a mature teratoma, with a 5 year survival of around 86% [53]. This is worse for a patient with an immature teratoma, with a survival rate of about 50-70% [9, 53]. There is a benefit from aggressive resection in these tumours [53, 54].

#### **1.3.4 OTHER TUMOURS**

In addition to the tumours listed, there are many other histological types. The list provided above covers all the major tumour types. Rare tumours provide a particular challenge in both diagnosis and management.

## 1.4 TUMOUR LOCATIONS

Different tumours can occur in different regions of the brain, and this affects diagnosis and prognosis.

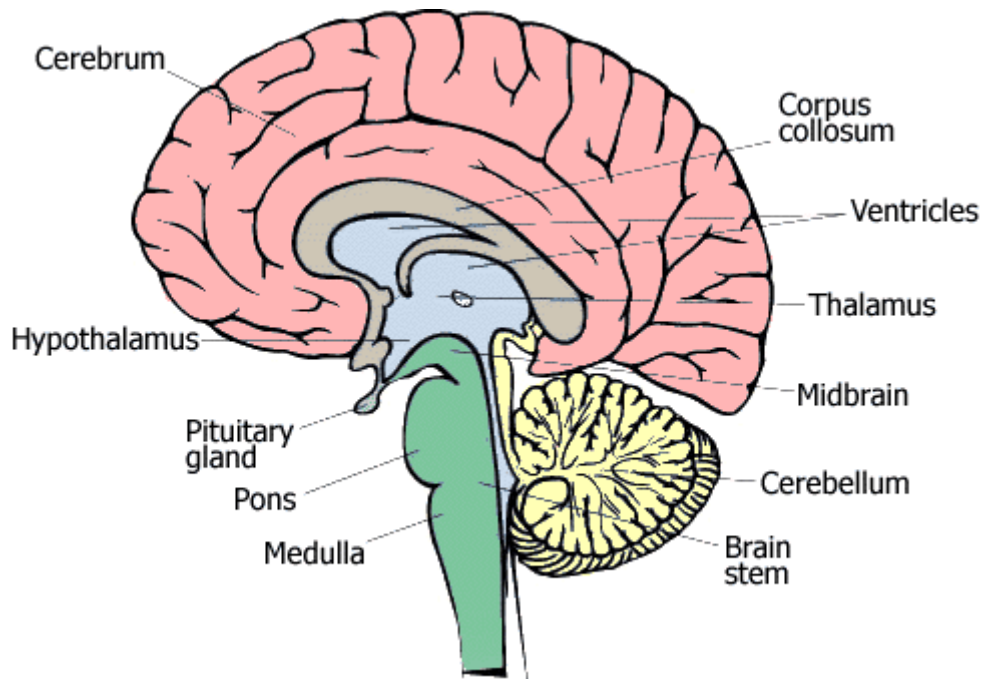


Figure 3: Brain diagram showing all major regions [55]

The following is a list and description of the major regions of the brain, relevant to this thesis:

- Supratentorial regions:
  - The cerebrum – this is the largest area of the brain and is made up of 2 hemispheres. Each hemisphere is subdivided into lobes: frontal, temporal, occipital and parietal. The cerebrum is largely concerned with mental functions such as thinking and memory, along with motor function and sensation.
  - Pineal gland – this is a small endocrine gland that produces melatonin, which affects the sleep/wake cycle.

- Pituitary gland – this is a small endocrine gland that secretes hormones that regulate homeostasis.
- Thalamus – amongst other functions, the thalamus plays an important part in the regulation of the sleep/wake cycle and is involved in level of awareness.
- Hypothalamus – this acts as a link between the nervous system and the endocrine systems. This is performed via the pituitary gland.
- Optic pathway – information about an image is transmitted via the optic nerves, these meet and cross at the optic chiasm. The chiasm is at the base of the hypothalamus; at this point the information coming from each eye is combined, split and, later, processed.
  
- Infratentorial:
  - The cerebellum - this is concerned with coordination and with balance.
  - The brain stem – this is at the base of the brain and connects it to the spine. It controls the functions that are essential for maintaining life: blood pressure, breathing and heart beat.

### **1.4.1 DISTRIBUTION**

The location of a lesion affects the type of tumour considered in diagnosis. In the adult population most brain tumours occur in the cerebral hemispheres.

This, however, is not the case in the paediatric population. Tumours in

children commonly occur infratentorially, in the brain stem or cerebellum, with around 50% of reported brain tumours being reported in these locations.

Around 20% are in the suprasellar/sellar region; this refers to tumours above the sella turcica (a saddle shaped decompression in the sphenoid bone). The remaining 30% occur in other supratentorial locations.

#### **1.4.2 CEREBELLAR TUMOURS**

Tumours that occur in the cerebellum are usually confined to 1 of 3 types:

- Pilocytic Astrocytoma
- Medulloblastoma
- Ependymoma

Although, other tumours, such as ATRTs [56] and high grade gliomas, can also occur here, amongst other rarer tumours.

#### **1.4.3 BRAIN STEM TUMOURS**

Most commonly types of astrocytoma occur in this region of the brain. There are either high or low grade:

- Diffuse Pontine Glioma (DPG)
- Tectal Plate Glioma (TPG) – assumed to be focal low grade glioma
- Focal astrocytoma of various grades

#### **1.4.4 PINEAL REGION TUMOURS**

3-8% of childhood brain tumours occur in the pineal region. This is a complex area to biopsy, with surgery carrying a risk of morbidity and mortality. This diverse group of tumours varies from the benign to the highly malignant, with highly different treatment requirements.

The most common pineal region tumours are germ cell tumours (GCTs):

- Germinoma
- Teratoma (mature and immature)
- SGCT

The other major group of pineal tumours arise from pineocytes:

- Pineoblastoma
- Pineal parenchymal tumour of intermediate differentiation (PPTID)
- Pineocytoma

Astrocytomas can also occur around the pineal gland.

#### **1.4.5 OPTIC PATHWAY TUMOURS and NEUROFIBROMATOSIS TYPE 1**

3-5% of childhood brain tumours are optic pathway gliomas [57]. Of these, approximately 25% are confined to the optic disc and nerve and 40-75% involved the chiasm. These are most common in the first decade of life, with approximately 75% being diagnosed at this age [58].

Neurofibromatosis Type 1 (NF1) is a familial condition which predisposes the carrier to developing low grade gliomas. These tend to be present in the optic pathways or chiasm and are more indolent than other low grade gliomas occurring in these locations [59-63]. If a diagnosis has been made using general diagnostic criteria for NF1 [59-61, 63] and a slow growing lesion is seen in the optic pathways/chiasm a biopsy is not usually performed as this is enough for a diagnosis [62, 64]. These tumours tend to be observed rather than treated aggressively [62].

## **1.5 CURRENT STATE OF MRS**

To date there have been several studies published relating to the use of MRS in the assessment of brain tumours, and these have shown the promise of this technique in this area [29, 65]. MRS has been used to improve diagnostic accuracy [27, 65], grading tumours [66-68], assessing for the presence of prognostic markers [69], and offer guidance for surgical intervention [70].

A much more limited number of studies have been performed in the paediatric population, which have also shown the benefit of using MRS to aid in the characterisation of tumours [71-73]. The number of studies achievable in the paediatric population has been hindered by small numbers of cases. Brain tumours are not common in children and thus only small groups are available for study. Much of the work published is in the form of case reports or a small series of cases. This leads to the need for larger multicentre studies, which introduces new problems. Multicentre studies need to be subject to strict protocols that are followed rigorously in order to allow for the data between institutions to be analysed together.

Much of the published data is also from MRS collected at a longer echo time (chapter 2.5); this leads to a loss of information from certain metabolites, lipids and macromolecules. The signals lost at longer echo times have been shown to be useful in the characterisation of tumours in studies collected at shorter echo times [66, 67, 71, 72, 74-76] .

## **1.6 CURRENT USES OF MRS IN BRAIN TUMOUR RESEARCH**

When a patient has a suspected brain tumour they traditionally have an imaging evaluation. This is performed either by CT or MRI scan. Contrast-enhanced MRI has been shown to offer a higher diagnostic accuracy than CT [77-79]. However, while MRI is very good at detecting the presence of lesions, it does not have a high diagnostic accuracy, with problems in the diagnosis of many tumours [80]. An improvement in accuracy has been shown to be possible by the addition of MRS to the standard MRI study [81]. One study using a mixed age group quotes an increase in diagnostic accuracy of indeterminate brain lesions from 55% to 71% when comparing MRS with MRI [27]. In another study, 104 out of 105 spectra were correctly identified by using 'leave-one-out' discriminant analysis on MRS data. This can be compared with conventional preoperative diagnosis methods, which misclassified 20 out of 91 tumours that were analysed [69]. In addition to this, conventional MRI offers us little information on the prognosis of tumours [82], little information about the grade of the tumour [74] and no information with regards to the biology of the tumour [83]. Conventionally, this is achieved by taking a biopsy sample and processing it using histopathology. This can lead to a sampling error in heterogeneous tumours, which may be reduced by using techniques such as MRS to target active tumour tissue [29, 70, 84]. Also, since all tumours do not require surgery as part of their curative treatment [9, 85], it would be better to remove unnecessary risks associated with surgery for these patients.

To date, many studies have been performed to assess the utility of MRS in adult patients in the diagnosis of both tumours and neurological disorders [27, 29, 30, 65-68, 84, 86-97]. There are a more limited number in the paediatric population [28, 71, 73, 75, 76, 86, 98-107]. Adult studies have shown the considerable promise of MRS as a method to diagnose and characterise tumours and also as an aid to assist in the understanding of the biology of these tumours.

Most studies using MRS use ratios between NAA, Cr and Cho as their major discriminating factors, as these appear to be the metabolites that alter by the greatest measureable amount in tumours compared with 'normal' brain, and these also vary strongly between tumour types. A common finding described is an elevated signal arising from Cho, either relative to water [87, 90, 94, 108-111] or in ratio to Cr or NAA [66, 70, 84, 87, 97].

Cho is a marker of cell turnover and is therefore elevated in tumour tissue. It has frequently been used to differentiate between tumour types that look similar using conventional MRI [90]. Cho/Cr is elevated in nearly all tumours [84]. This has also been used to grade tumours, with higher levels being reported in more aggressive tumours [68, 87, 97]. The ratio between Cho/Cr is such a strong indicator of cancerous tissue, that it has been used in one study to guide biopsies, leading to a success rate of 100% in obtaining tissue useful for histopathological processing [70]. NAA/Cho is also altered in glioma tissue [84, 87], and this can also be used to differentiate between high and low grade gliomas [66, 84]. Cho ratios have also been used in monitoring

treatment response [108, 110, 111] and in determining the difference between recurrence and radiation changes post radiotherapy [109].

NAA is another metabolite closely linked with tumour characterisation. It is a marker of neurons and is, therefore, usually higher in healthy brain tissue when compared with tumour tissue [87, 90, 94, 96, 97, 112]. This is lower in high grade tumours compared with low grade tumours, and this can be used to differentiate these either referenced to internal water [90, 94, 96] or in ratio to Cr [84, 97]. NAA and Cho can be used in combination as a ratio to target areas of active tumours tissue, the area where this is highest has been shown to be the densest area of infiltration of tumour cells [84], this ratio has also been shown to alter prior to progression [110].

Creatine is often used as an internal concentration reference as it is usually present in brain tissue. This is not always the case in glioma tissue though [94], where it is decreased. It is often absent entirely in high grade gliomas [94], and can therefore be used as a method of grading these tumours. This can mean that it is more useful to use Cho or internal water as a reference rather than Cr.

Signals arising from Lipids and Macromolecules are not usually seen in healthy brain tissue, but are elevated in tumour tissue [66, 68, 84, 94, 110, 113]. These are higher in aggressive tumours than benign and are often linked with malignancy [66, 68, 84, 94], and have also been shown to increase before progression [110]. LMM have also been confirmed using ex vivo sampling as a method to grade tumours [113].

One of the most prominent peaks associated with LMM signals is at 1.3/1.4ppm and 0.9ppm. This peak often overlaps with the doublet assigned to Lac, leading to some mis-assignment and inaccurate quantitation. This can be resolved by using an intermediate echo time of ~135ms, at this point Lac is inverted and the LMM signals have decayed. This inversion has been seen in glioma tissue [68]. Lac has been repeatedly seen in glioma tissue [68, 84, 89, 93, 94, 110]. As with LMM concentrations, Lac has been used in the grading of tumours, in particular in the grading of gliomas [68, 84, 93, 94]. One study saw only Lac in LGGs, whereas LMM signals were strong in higher grade tumours [94]. When performed on the cysts that are associated with a tumour, it has been shown that Lac is of use in the grading of tumours. Higher levels of lactate within a cyst pertain to higher level of aggression of the lesion [89].

Another metabolite present at short echo times, but not long, is mIns. This has been shown to be very important in the analysis of glioma tissue [67, 87, 90]. Lower grade gliomas show an elevated mIns signal [67, 90], whereas this is decreased in higher grade gliomas [67].

Other smaller metabolites not seen at long echo times include Glu, Gln, sIns and Tau. These have all been seen in tumour tissue [66, 87, 108], and have been useful in determining prognosis [108] and in grading tumours [66, 87].

## *PAEDIATRIC STUDIES*

These findings have been echoed in studies performed on a paediatric cohort. Cho is repeatedly elevated in higher grade tumours and is useful for grading purposes [74]. NAA can also be used for grading, being higher in controls [72, 105] and in lower grade tumours [98] compared with more malignant lesions. Both of these metabolites have also been used to predict response to treatment [101, 114]. Percentage change in Cho concentration can be used to predict progression [101, 114], as can the maximum Cho/NAA ratio at diagnosis to predict survival time [107]. Creatine has again been shown to be significantly lower in tumour tissue when compared with normal surrounding brain tissue [86], this is especially low in glioma tissue [71, 98].

Again, LMM signals have been shown to be elevated in tumour tissue [72, 74, 75, 115, 116] and have been used in both diagnosis [72, 74, 115] and monitoring treatment response and progression [75, 116]. A conjunction with the signal arising from Cho, the best diagnostic accuracy [74] and independent predictor of survival [75] was achieved.

Not all tumours arising in adults occur in children and vice versa, and as such there are some findings that can only be detected in a paediatric cohort.

Approximately one half of childhood brain tumours occur in the posterior fossa [41]. The three most common histopathological tumour types in the cerebellum are PA, medulloblastoma and ependymoma.

Cr concentration is especially low [71] in PAs and they usually have a prominent NAA peaks present at 2.0ppm and a high Cho concentration [73] .

The NAA peak is decreased in ependymoma and medulloblastoma spectra compared with PA spectra [71, 73, 100]. The presence of a large concentration of Cho in medulloblastoma spectra leads to the ratio NAA/Cho being able to be used to distinguish medulloblastoma from other posterior fossa tumours [73, 100].

Ependymoma spectra exhibit a very strong peak assigned to mIns [98, 99]. This can be used as a major distinguishing feature of the spectra associated with these tumours. The ratios mIns/Cho and mIns/NAA are lowest in medulloblastoma spectra [72, 99].

The presence of Tau in the medulloblastoma spectra is another distinctive characteristic of these tumours [71, 96, 98, 100]. This resonance is not seen in a large concentration of any other posterior fossa tumour, although it has been seen in germinoma spectra [71].

Other features seen in these 3 tumour types include PAs having a higher Lac/Cho ratio compared with the other 2 tumours types [73]. This echoes observations made with gliomas showing a high Lac concentration [68, 84, 89, 93, 94, 110]. Glx has also been reported as being elevated in PAs compared with other tumour types [72].

Another, less studied tumour type, more common in children, is the diffuse pontine glioma. This is a tumour with a particularly dismal prognosis [42] and little is understood about their biology due to lack of biopsy tissue. MRS has shown a strong resonance due to mIns and less pronounced increase in Cho compared with other tumours, leading to an elevated ratio mIns/Cho [72]. They also show a low ratio for Glx/Cho [72]. It is tumours such as these, where biopsy carries too large a risk that MRS can be of the most use.

# **AIM AND OBJECTIVES**

## **AIM**

The aim of this body of work is to improve the non-invasive characterisation of childhood brain tumours

## **OBJECTIVES**

1. To assess short echo time (TE=30ms) MRS for the characterisation of childhood brain tumours, in particular the metabolites not easily quantitated in long echo time (TE=135ms) MRS
2. To compare MRS peak height ratios with metabolite concentrations for the diagnosis and characterisation of childhood cerebellar tumours
3. To apply these analysis methods to brain tumours of the pineal gland and brain stem, for which non-invasive diagnosis would be particularly useful
4. To explore the ability of MRS to predict the clinical and biological behaviour of pilocytic astrocytomas

## **MAJOR CONTRIBUTIONS**

1. A simple classifier for childhood cerebellar tumours based on differences between peak height ratios [99] (chapters 4.2)
2. A comparison of methods between a simple peak height classifier and a more sophisticated method based upon metabolite and LMM concentrations as given by LCModel™ (chapters 4.3 and 4.4)

3. An analysis of the differences in spectra between childhood germ cell tumours of the pineal region and other tumours occurring in this area [117] (chapter 5)
4. An analysis of childhood brain stem tumours with an emphasis on diffuse tumours of the pons [118] (chapter 6)
5. An analysis of the variation between spectra of pilocytic astrocytoma occurring supratentorially and infratentorially [119] (chapter 7)
6. Determining preliminary prognostic markers for supratentorial pilocytic astrocytomas [119] (chapter 7).

## **OVERVIEW OF RESULTS**

In chapters 5, 6 and 7, short echo time MRS is studied in a series of important clinical scenarios involving children with brain tumours. The ability of the technique to aid non-invasive diagnosis, provide prognostic biomarkers and improve treatment monitoring of childhood brain tumours is investigated. In particular, the role of metabolites which are not well quantified at long echo times is determined. The emphasis of the work is on providing guidance to clinicians in the use of MRS.

The strategy starts with the development and evaluation of simple classification schemes for cerebellar tumours at diagnosis, chapter 4. The aim of this chapter is to determine the ability of short echo time MRS to characterise a specified set of childhood brain tumours and determine the feasibility of providing a diagnostic scheme for clinicians. Cerebellar tumours were selected as the test-bed for this part of the work, since they have a

relatively high incidence and surgery usually forms part of the treatment making a definitive histopathological diagnosis available. Previous MRS studies have also been reported for this tumour group allowing important comparisons to be made.

Two approaches to MRS analysis are used in chapter 4. The first approach was designed to be used entirely in a clinical setting, where sophisticated MRS processing and analysis tools are not readily available (chapter 4.2). The method relies on measuring MRS peak heights of major metabolites from spectra produced by software available on the MR scanner. This scheme was developed using data collected using a single MR scanner (chapter 4.2.1) then evaluated prospectively using data collected from more than one centre (chapter 4.2.2). The classification scheme was also re-optimised using the entire data available (chapter 4.2.3). The second approach used a more sophisticated MRS analysis in which a commercially available software package (LCModel™ [120]) was used to quantify the concentrations of a larger number of metabolites and these were used to provide a simple classifier for diagnosis (chapter 4.3.1). This scheme was also evaluated prospectively on the same dataset that was used to evaluate the classifier based on peak heights (chapters 4.3.2).

Having investigated short echo time MRS on a group of tumours with a histopathological diagnosis, the technique was applied to brain tumours in the pineal gland (chapter 5) and brain stem (chapter 6). Developing non-invasive diagnostic techniques for tumours in these locations is of particular

importance, since surgery poses significant risks. Furthermore, the lack of tumour tissue for research makes non-invasive techniques for providing information on the biology of these tumours particularly valuable. This is illustrated in chapter 6 where the ability of two distinct types of diffuse pontine glioma a particularly poor prognosis and poorly understood tumour, is investigated and two distinct types may be defined by their MRS profiles.

The final clinical study of the thesis concentrates on one specific diagnostic type, pilocytic astrocytomas (chapter 7). A number of important biological and clinical problems exist for this tumour group beyond non-invasive diagnosis for which MRS could be an important tool. The non-invasive detection of variations between tumours in different locations of the brain; the measurement of prognostic biomarkers and the detection of early markers of treatment failure are investigated.

## **CHAPTER 2: MAGNETIC RESONANCE**

### **SPECTROSCOPY**

The NMR phenomenon was first described in 1946 by both Felix Bloch [121] and Edward Mills Purcell [122], who later shared the Nobel prize in physics in 1952 for the discovery. Since then, NMR techniques have been increasingly used in both research and clinical settings.

Two important applications of the NMR phenomenon are now in both clinical and research use: Magnetic Resonance Imaging (MRI) and Magnetic Resonance Spectroscopy (MRS). In MRI, the protons present in tissue water are detected and these are used to generate a structural image. In MRS, it is the protons present in metabolites and macro-molecules other than water that are of particular importance.

A basic understanding of the fundamental principles of magnetic resonance (MR) is vital for understanding the role of MRS in a clinical setting. The following section outlines the basic principles of MR, equipment used and how it is applied in a clinical and research setting [123]. A full account of NMR physics and instrumentation is beyond the scope of this thesis, there are many standard texts which cover this in more detail [123, 124].

#### **2.1 THEORY OF THE NMR PHENOMENON**

Cells in the human body contain up to 90% water, this leads to a large prevalence of hydrogen atoms in the human body. The hydrogen nucleus is a

single proton, which has a positive charge and possesses a magnetic quality called nuclear spin. Other atomic nuclei, including carbon-13 and phosphorus also possess nuclear spin and can be used in an MR experiment, but hydrogen is usually the preferred choice. Hydrogen is the most abundant nuclei in the human body that possess a nuclear spin.

In the absence of an external magnetic field, the directions of nuclear spin vectors, usually known as magnetic dipole moments, are oriented randomly. However, when a body is exposed to a strong static external magnetic field ( $B_0$ ), the magnetic dipole moments will align with this external field and they will begin to precess about the main direction of the field. An oscillating magnetic field is generated by the precessing net magnetisation. The frequency of this precession, the Larmor frequency, can be calculated via the Larmor equation:

$$\omega_0 = \gamma B_0$$

*Equation 1: The Larmor Equations*

*$\omega$  = frequency;  $\gamma$  = gyromagnetic ratio;  $B$  = magnetic field strength*

Under these conditions, known as the ground or equilibrium state, there exist marginally more spins aligned parallel to the field, in a low-energy state, than anti-parallel, in a high-energy state.

This excess number of magnetic dipole moments aligning parallel with the field produces a potentially observable bulk magnetization for a sample of spins when placed in an external magnetic field and it is known as the

macroscopic or equilibrium magnetization. Using a second electromagnetic field, oscillating at radiofrequencies perpendicular to the main field, these nuclei are pushed out of alignment, moving the net magnetization to a different angle. As these nuclei drift back to align with the main field they emit a detectable radiofrequency. Protons in different environments, i.e. in different tissue types, will realign at different speeds, and thus they will have a differing T1 relaxation time. When the spins precess in the transverse plane they induce an oscillating current that can be detected by the receiver coil. This signal corresponds to an exponentially decaying sinusoid in the time domain, and is called the Free Induction Decay (FID).

The energy difference between the two spin states is proportional to the frequency. This frequency is proportional to both  $B_0$  and the gyromagnetic ratio, equation 1. The gyromagnetic ratio is characteristic of a given nuclei, and is relatively high for hydrogen. Thus, a nuclei with a high gyromagnetic ratio will lead to a larger energy difference between spin states. Hydrogen has a relatively large gyromagnetic ratio, leading to a larger energy difference and therefore improving the sensitivity of the technique. This, in addition to the relatively high abundance in the human body, is why  $^1\text{H}$ -MRS is the most commonly used for of MRS.

One factor affecting the strength of this signal is the number of nuclei that give rise to it, in order to increase the signal-to-noise ratio (SNR) several data acquisitions are recorded and the resulting signal is averaged over all of these.

The relaxation rate can be characterised by two time constants known as T1 and T2.

T1 (longitudinal) relaxation time describes the recovery of the z-component on the net magnetisation vector, while the T2 (transverse) relaxation time describes the decay of the xy component.

T1 (longitudinal) relaxation time is the time it takes to recover 63% of the equilibrium magnetisation [123]. It is related to the transfer of energy from a nuclear spin to the surrounding environment, this is usually referred to as a lattice and hence this can sometimes be referred to as spin-lattice interactions. At equilibrium point, all the magnetisation is aligned with the external field.

The T2 relaxation time is related to the effect that nuclear spins have on each other; these are often referred to as spin-spin interactions. This refers to the loss of phase coherence of the spins as they interact via their oscillating magnetic fields. The slight change in B experienced by the proton cause its Larmor frequency to change (Equation 1). The result of this is that the precession of spins moves out of phase and this loss of phase coherence results in a reduction in the transverse magnetisation. In general, T2 is greater than or equal to T1.

In an ideal model, the FID will decay exponentially with T2. Spins will dephase due to molecular interactions as well as an inhomogeneous magnetic field. These inhomogeneities in the external field cause the field to

have slightly different strengths at different locations in a sample. This causes the Larmor frequency to vary across the body, which leads to destructive interference. This interference, in turn, shortens the FID. The observed decay of the FID is described by a time constant known as  $T2^*$ .  $T2^*$  is always shorter than  $T2$ . Additional coils can be used to compensate for these inhomogeneities. These are referred to as shim coils and the current in these coils can be altered to improve the magnetic field distribution. This process is known as shimming.

## **2.2 MAGNETIC RESONANCE SPECTROSCOPY (MRS)**

Metabolites, and other resonances, can be distinguished in a spectrum due to a feature known as chemical shift. The chemical environment of a given nucleus will effect the resonance frequency, the chemical shift is a measure of this dependence [123].

A synthesised proton MR spectrum is shown Figure 4, this spectrum was produced using software that uses the density matrix formulation of NMR [125]. Each of these peaks is 'fixed' at a given frequency [123]. This is shown as a fixed position on the x-axis, which shows the chemical shift. The chemical shift on this axis is parts per million (ppm) of  $B_0$ . Some of the signal is seen as being inverted, this is due to not all of the signal being refocused at an echo time of 30ms.

This can be explained using an example, such as lactate which has a J-coupling of 14Hz. To fully refocus something with a J-coupling of 14Hz you

need an echo time of  $1/14$ . For lactate this will be a TE = 0.270s or 270ms or multiples of this, i.e. TE = 0, 270, 540ms etc. If a TE of half of this is use, i.e. 135ms for lactate, then the peak/s will be inverted. TE of 30ms is close to 0ms, thus a majority of the signal from lactate will be refocused, but a small component will appear inverted about the x-axis.

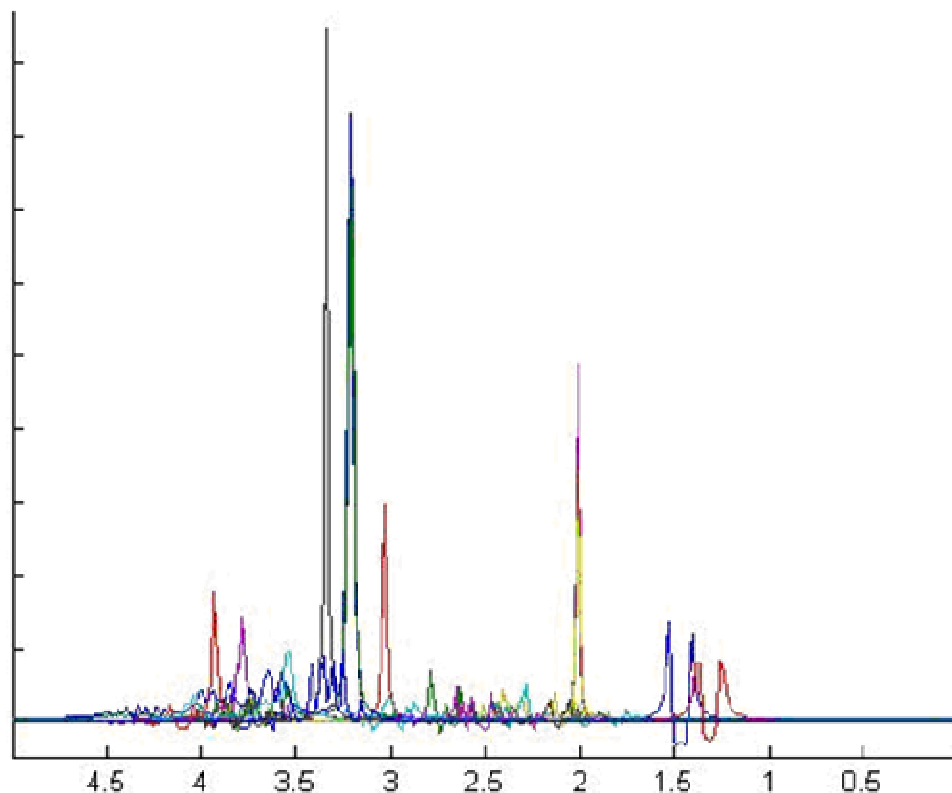


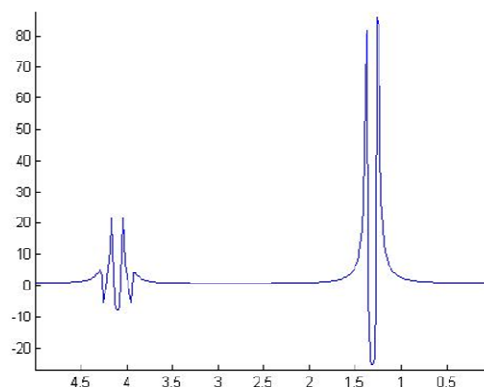
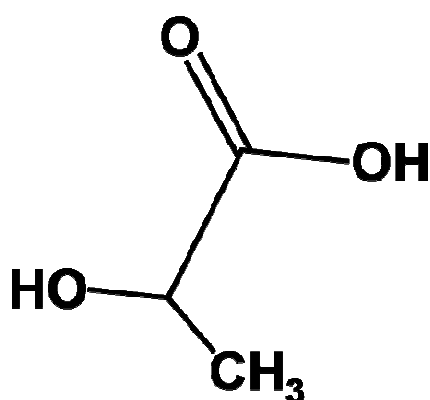
*Figure 4: Synthesised in vivo  $^1\text{H}$ -MRS spectrum, the region is limited to 0ppm – 5ppm. Each metabolite's individual spectrum is shown in a different colour.*

Simple metabolites may just give a single peak. Other metabolites lead to a combination of singlets and multiplets.

Nuclei that are connected with covalent bonds will experience some effect from each other's effective magnetic field. This effect can be detected in the MR spectrum between non-equivalent nuclei. This effect is known as J-

coupling, or spin-spin coupling, and is seen in the MR spectrum as a splitting of peaks [123]. An example of this effect can be depicted by the doublet shown by lactate (Figure 5)

Lactate has three magnetically equivalent methyl protons coupled to a single methine proton. Since the methyl protons are magnetically equivalent they do not produce any splitting between themselves, but they do experience an effect from the methine proton, this results in the doublet seen at 1.31ppm. The methine proton experiences three spins, all of which have the same coupling constant. The result of this is the line at 4.10ppm splitting into four (a quartet), with a ratio of 1:3:3:1 (figure 5b).



(a)

(b)

Figure 5: (a) molecular structure of lactate; (b) <sup>1</sup>H spectrum of lactate

From the pattern of the resulting peaks we can determine which metabolites are being seen in a spectrum. This can be achieved by using a combination of the known spectra of specific individual metabolites (Figure 4). These known spectra can then be used to 'fit' to the experimental spectrum, and this can give information regarding which metabolites are present and in what

abundance. All metabolite concentrations have to be calculated in reference to a known peak; usually water.

MRS can be performed both in vivo and in vitro. Spectra taken in vitro can be used to aid in the interpretation of those taken in vivo. In the case of in vitro, or ex vivo, NMR, the tissue is frozen at the time of surgery using liquid nitrogen. This tissue can then be transported to the spectrometer for analysis. The field strength used to obtain in vitro spectra can be as high as 21T compared to the usual 1.5T used clinical practice. A higher magnetic field strength will lead to better signal-to-noise, resulting in a clearer spectrum with greater peak resolution. In addition to this, leading to a spectrum with sharper peaks, that can be more easily assigned to metabolites.

## **2.3 CLINICAL MRS**

### **2.3.1 PULSE SEQUENCES**

A spin-echo is the reappearance of the MR signal after the initial FID has decayed. To generate a spin-echo signal, a  $180^\circ$  pulse is applied after the  $90^\circ$  pulse. Local variations in the field cause some spins to precess faster than others, this leads to a spread of phases at the  $180^\circ$  pulse. This refocusing pulse reverses the order, but not the direction, of the precession. Thus, those spins that were precessing faster are now behind, in the sense of phase, the lower frequency spins. After a period of time, equal to that between the  $90^\circ$  and  $180^\circ$  pulses, the spins realign to form an echo. This process can be repeated by applying subsequent  $180^\circ$  pulses, creating an 'echo train' of signal. The  $180^\circ$  pulse does not cause all of the protons to fully

rephase, due to the inhomogeneous magnetic field; therefore the full transverse magnetisation is not fully recovered. The pulse does cause a proportion of the original phasing to be recovered. Therefore, the maximum intensity at each pulse is limited by an exponential decay curve, this has the decay constant  $T_2$ . This value is always greater than  $T_2^*$ , since  $T_2^*$  has components from both fluctuations in the magnetic field within the body and also non-uniformities in the magnet itself.

This can be used to obtain localised MRS data, by only exciting and refocusing signal within a desired volume. The two most common methods, used in single-voxel spectroscopy (SVS), are stimulated echo acquisition mode (STEAM) [126] and point-resolved spectroscopy (PRESS) [127]. For all the work published here, the PRESS sequence is used.

The PRESS sequence [127]:

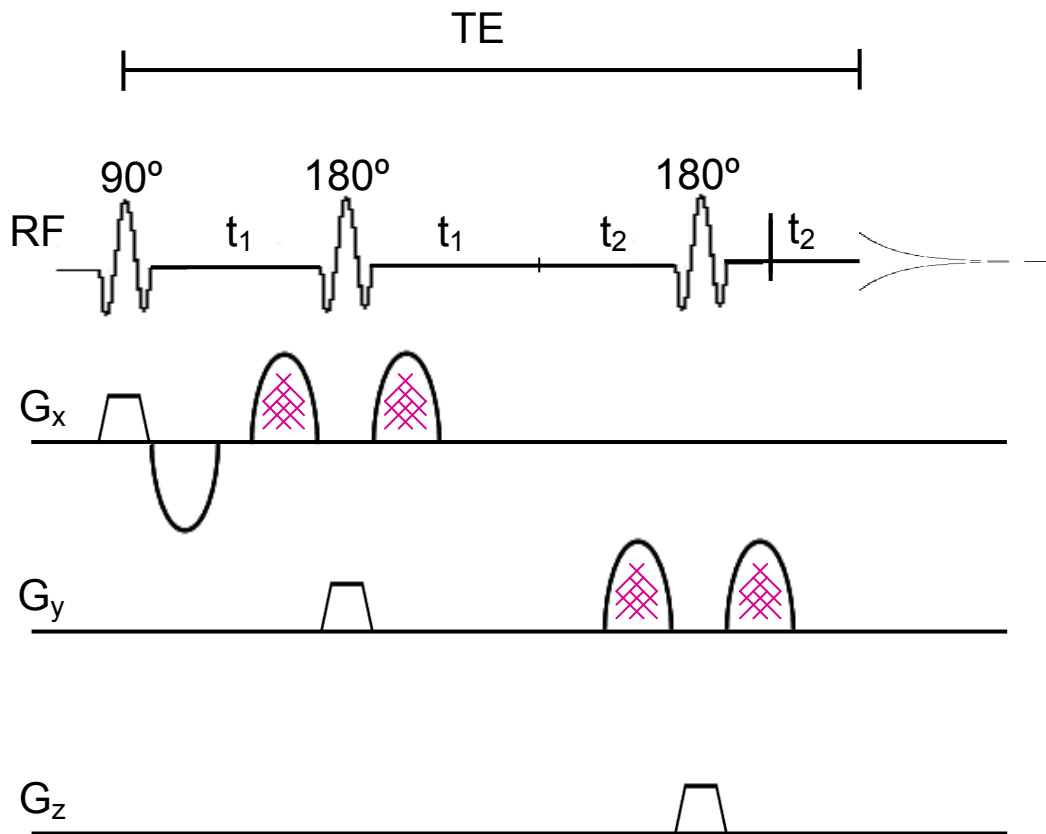


Figure 6: The PRESS Sequence

*The use of crusher gradients (highlighted in pink) to flank the 180° refocusing pulses will ensure that there is selection of the desired coherences, while destroying all others.*

PRESS is a double spin-echo method, where slice-selective excitation is used in combination with two slice-selective refocusing pulses (figure 6). The initial 90° pulse is followed after a time period  $t_1$  by a 180° pulse. This is followed by a spin-echo at  $2t_1$ . The second 180° pulse is applied to refocus this spin-echo at a delay time  $2t_2$ . This leads to a final spin-echo appearing at a time  $2t_1 + 2t_2$ , this is equal to the echo time of PRESS ( $TE = 2t_1 + 2t_2$ ). The first spin echo only contains signal from the column that is the intersection between the two orthogonal slices selected by the 90° pulse and the first of the 180° pulses. The second spin-echo only contain signal from the intersection of the

three planes selected by the three pulses, this results in the selection of the desired volume. Signal outside of the volume of interest is either not excited or not refocused; this leads to rapid dephasing of the signal by the “TE crusher” magnetic field gradients. This block of three pulses ( $90^\circ$ - $180^\circ$ - $180^\circ$ ) is successively repeated. The repetition time (TR) refers to the time interval between  $90^\circ$  pulses and the time between the  $90^\circ$  pulse and signal sampling is referred to as the echo time (TE).

### **2.3.2 WATER SUPPRESSION**

The metabolites of interest have much lower concentrations (mmol/l) than that of tissue water (1-10mmol/l). This leads to a signal at 4.7ppm dominating the  $^1\text{H}$ -MR spectrum. In order to detect the metabolite signal, it is necessary to suppress the large signal from water [123].

One method in which to achieve this is by applying sequences of short, high amplitude RF pulses with delays between. This allows for frequency selective excitation. These sequences are designed to allow the metabolite resonances to rotate into the transverse plane, thus allowing for signal detection, while the water is returned to the longitudinal axis, rendering it unobservable. While this method is imperfect, it does perform well and allows for the majority of the signal from the water molecules to be removed [123].

### **2.3.3 MRS SIGNAL PRE-PROCESSING**

The FID consists of signal from a variety of sources, including those from all metabolites, LMM and macromolecules. In addition to this, there will be components from noise and, potentially, a signal due to residual water. Several steps can be undertaken in order to maximize data quality and remove any irrelevant information.

#### *FREQUENCY ALIGNMENT*

Spectra are referenced by assigning a known chemical shift to a metabolite. In scanner processed spectra the spectra will be aligned to the water peak at 4.8ppm. This is generally stable at 4.8ppm; however it does have a sensitivity to temperature and pH. The molecular location of the water can vary between intercellular and extracellular water, which can also lead to some line broadening of the water peak.

In spectra processed by LCModel™ [120] there are two options on processing, dependent on whether the region of interest is healthy brain or tumour. In the case of healthy brain, the spectrum is aligned to the NAA peak at 2.0ppm, which is generally stable and the largest peak in health brain in the region 0-4ppm. In tumour spectra, the spectrum is aligned with a combination of peaks and shifted accordingly to allow for the variation seen in tumour spectra.

### *PHASE AND LINESHAPE CORRECTION*

A water unsuppressed spectrum can be used to correct the phase of a spectrum, by dividing the water suppressed signal by the phase term of the water unsuppressed signal. This step corrects for eddy currents, which are caused by imperfections in the instruments.

Most quantification tools model the spectrum as a sum of lorentzian lineshapes. In practice, this is not achieved in vivo due to the effects from eddy currents and inhomogeneities in the magnetic field. Eddy currents cause a time varying magnetic field, this distorts the MR resonances. Time varying magnetic fields are the same for all resonances, thus the unsuppressed water spectrum can be used to correct for these contributions. Contributions due to inhomogeneities can be removed by dividing the water suppressed FID by the unsuppressed envelope.

### *RESIDUAL WATER*

In the region 1-4.2ppm residual water is not generally a problem; this is the region of interest for the scope of this thesis. In regions closer to the water peak, there are several automated post acquisition methods, most of which use a single value decomposition of the FID signal [123].

### *BASELINE CORRECTION*

Most spectra will exhibit sharp metabolite peaks superimposed upon a baseline of broader components, mainly arising due to contributions from

macromolecules. Many analysis tools use prior knowledge of these macromolecules to account for this signal.

#### **2.3.4 TYPES OF MRS LOCALISATION: SVS Vs MULTIVOXEL**

The 2 main approaches of collecting MRS data: SVS and multivoxel (also known as chemical shift imaging (CSI) or magnetic resonance spectroscopic imaging (MRSI)). SVS is performed by selecting a region of interest and placing 1 voxel (volume of interest) in this region. CSI is performed by placing a grid of voxels over the region of interest; this can be performed in 2D or 3D.

In a CSI examination, a grid of voxels is placed on the area of interest. This can then either be viewed as a matrix of spectra or as a colour map, with areas of high concentration of a selected metabolite (or ratio of metabolites) being graded.

CSI is particularly useful in detecting spread of disease beyond the obvious foci; this is of particular use in diffuse tumours [112, 128]. MRS can be used in surgical planning to guide biopsy [70], by targeting areas of active tumour in adults. It is also very useful post operatively, in the assessment of irregular shaped or large, heterogeneous lesions, to determine response to treatment and areas of recurrence [109, 110]. However, it is challenging to perform CSI at shorter echo times and thus the amount of information contained is limited. Also, long acquisition times are needed to obtain a good quality spectrum.

### 2.3.5 ECHO TIMES

In a spin-echo experiment a second RF pulse is applied after the initial  $90^\circ$  pulse, with a precession angle of  $180^\circ$  after a given delay time. A spin-echo can then be detected, this information can be collected at different echo times (TEs). In principle both the spin-echo time domain signal and the FID contain the same information about frequencies and intensities. However, the delay time between the 2 RF pulses used in the spin-echo experiment allows nuclear magnetisation to be manipulated and this can be used to create spatial localisation.

The timing of the different RF pulses used is determined by both TE and TR. TE is defined as being the time between the initial application of a  $90^\circ$  RF pulse and the peak of the echo. This results in a differing amount of metabolite information being present in the resulting spectrum. TR is defined as being the time between pulse sequences as applied to a single slice. SNR will be greatly improved by the collection of repeated measurements, thus TR results from the compromise between the desired SNR and the time for the taken for the experiment.

Signals from different metabolites have different rates of decay; this is due to the T2 value being dependent on the environment protons is found in. By collecting data at different echo times we obtain information from a different number of metabolites. At short echo times less metabolite signals have decayed, leading to more information being present in the spectrum.

However, this can be problematic due to overlapping peaks and the presence of signals from lipids and macromolecules.

Longer echo times ( $TE > 135\text{ms}$ ) allow for a more signal intensity to decay, resulting in fewer peaks and, thus, a clearer spectrum (figure 7a). However, this leads to the loss of potentially interesting metabolite information.

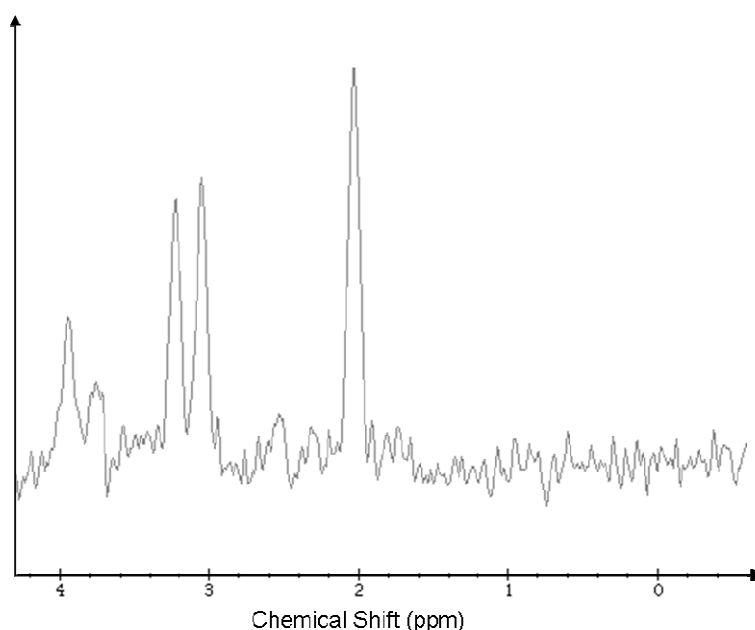


*Figure 7a: Example of a  $^1\text{H}$  spectrum taken at  $TE = 135\text{ms}$*

Signal due to small metabolites with strong  $J$  coupling decay at longer echo times, due to destructive interactions between resonances with  $J$ -coupled induced phasing. These include signals from Glutamate, Glutamine and myo-inositol (mIns). Lipids and Macromolecules can often dominate a short echo time spectrum, however these have short  $T_2$  decay times and are, therefore, not present in a long echo time spectrum.

Spectroscopy at a long echo time is particularly beneficial in certain regions, such as, between 2 and 2.6ppm. This region contains signals from NAA, Glu,

Gln, LMMs, as well as smaller metabolites such as GABA. Despite this benefit, problems can occur in the determination of NAA in a spectrum [129], usually, with concentrations often being overestimated. By using a longer echo time Glu, Gln, much of the LMM signals and those from smaller metabolites have decayed and, so, this peak is clear and the concentration is more easily determined. In addition to this, lactate is inverted at longer echo times ( $TE \sim 135\text{ms}$ ), and this can be more easily assigned.

However, this benefit of easy peak assignment and quantitation is offset by the lack of information present in a long echo time spectrum. Those metabolites which decay quickly are often of a lot of importance when it comes to analysing a tumour, and a short echo time spectrum could be beneficial. An example of a short echo time spectrum is shown in figure 7b, this spectrum was taken at the same time as that in figure 7a. Both spectra were of the same voxel and were taken using identical parameters with only the echo time varying between them.



























































































































































































































































































































